SENTINEL-1 BASED GROUND DEFORMATION MONITORING OVER ACTIVE OPEN-CAST MINING AREA IN TUBAY, AGUSAN DEL NORTE, PHILIPPINES USING STAMPS/MTI ANALYSIS

Monalaine M. Bermoy[1,2], Anlene Jane M. Eduava[1], Aj Webb O. Buenaflor[1]
[1]Department of Geodetic Engineering, Caraga State University, Ampayon, Butuan City, 8600, Philippines Emails: mmbermoy@carsu.edu.ph, anlenejane.eduava@carsu.edu.ph, ajwebb.buenaflor@carsu.edu.ph
[2]Caraga Center for Geo-informatics, Caraga State University, Ampayon, Butuan City, 8600, Philippines
Emails: mmbermoy@carsu.edu.ph

KEY WORDS: Sentinel-1, SAR, DInSAR, ground change detection

ABSTRACT: Interferometric Synthetic Aperture Radar (InSAR) is an effective technique for quantifying surface deformations using radar images. It is already well-established in international settings for different ground deformation mapping applications. This study then aims to utilize InSAR techniques for mapping ground deformations in a mining area through PSI and StaMPS/MTI analysis. The area considered in this study is an open-cast mining area in Tubay, Agusan del Norte, owned by the San Roque Mining Incorporation. A total of 153 Sentinel-1 satellite SAR acquisitions of the San Roque Mining Incorporation mining area, covering 2015-2020, were analyzed to generate velocity and time-series displacement maps. The time-series deformation rates showed subsidence from 2015 to 2016 and an uplift in the rest of the datasets. Overall, displacement rates present in San Roque Mining Incorporation in the 2015-2020 period are not alarming and are less likely to cause significant deformation. The idea behind this study is to introduce the practical use of available satellite SAR images and PS-InSAR methodology in quantifying displacements, detecting land movements, and assessing landscape changes for monitoring and managing mining environments.

1. INTRODUCTION

Through the years, mining activities have been the primary anthropogenic activity that causes topographic surface changes [1]. According to [1] and [2], surface mining is the primary reason for material displacement that causes land cover, watershed, and vegetation changes. Numerous advances in satellite imagery, e.g., Interferometric Synthetic Aperture Radar (InSAR), a processing chain that allows users to map the time-series ground deformation from SAR acquisitions [3], have increased the efficacy and reliability of gathered satellite data. Using Persistent Scatter Interferometry (PSI) analysis, researchers can monitor and quantify the earth's surface displacements over time and broader coverage than traditional ground-based surveying techniques [4]. Caraga Region currently has four active mining companies, one of which is the San Roque Metal Inc., located in the municipality of Tubay, Agusan del Norte, having a total area of 1079.50 ha. SRMI is an open-cast type of mining that requires large amounts of ores because of small concentrations of the minerals. During its operation, the residents filed numerous complaints and petitions to SRMI due to the environmental destruction and health impacts resulting from the company's alleged negligence [5]. Thus, assessing how much the topography has changed from 2015 to 2020 is of great significance in determining the level of degradation and land reclamation measures for post-mining.

The general objective of this study is to test the applicability and functionality of PSI and StaMPS/MTI analysis in detecting and quantifying the ground movement and displacement values in the Caraga mining setting. The specific objectives this study attempts to address are: (1) to quantify mean line-of-sight (LOS) velocities and (2) to map the time-series movement of line-of-sight (LOS) displacement using open-source packages and platforms.

2. METHODOLOGY

2.1. Study Area

The study area is San Roque Mining Incorporation, located at Barangay Binuangan and La Fraternidad, Tubay, Agusan del Norte, with coordinates; center latitude: 9.2057°N, center longitude: 125.5364°E, and having a sizeable area of 1080 hectares. The site has a mountainous terrain with an average height of 253-320 meters from mean sea level and a dispersed number of permanent structures.

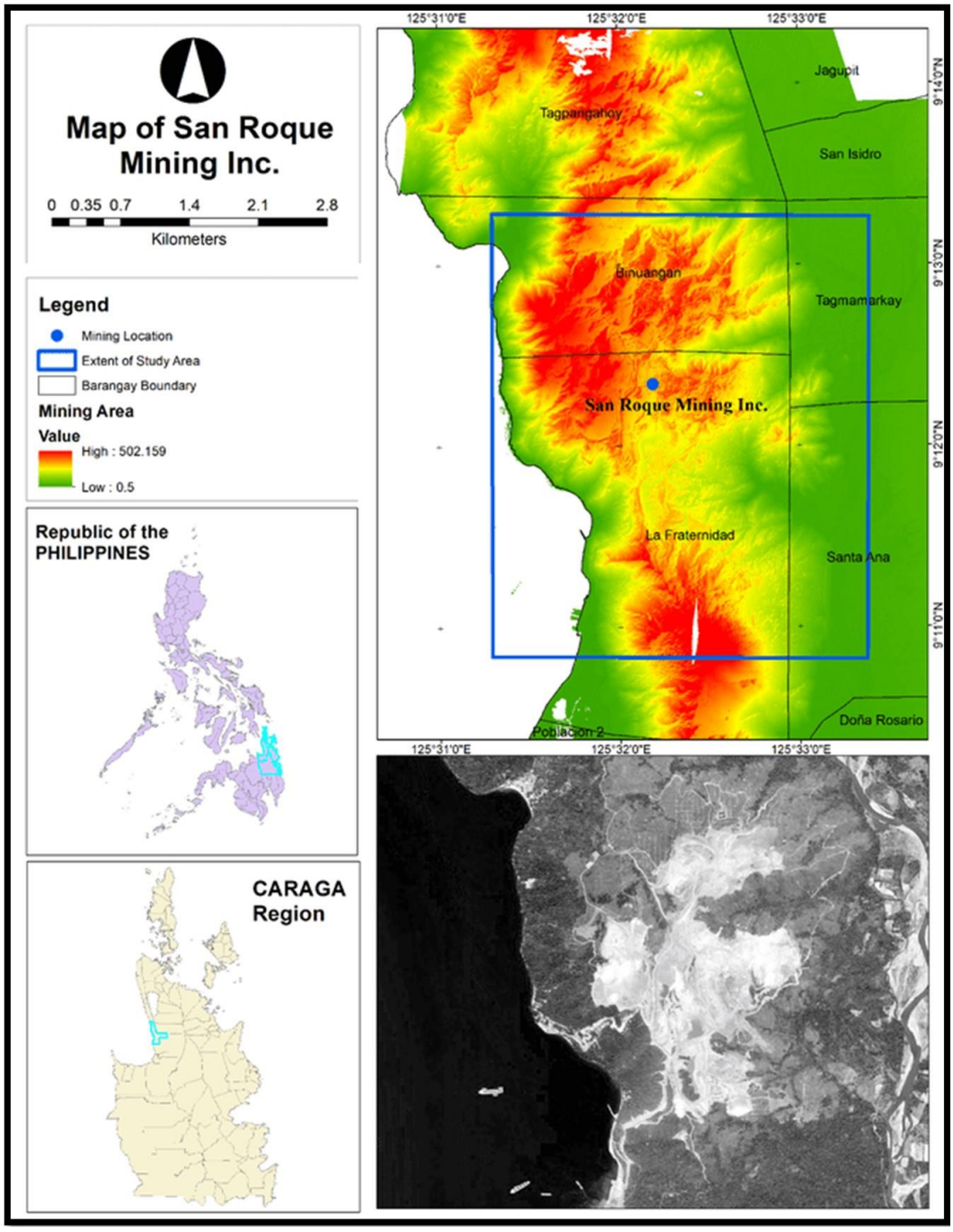

Figure 1 Map of the Study Area

2.2. Data Gathering

Sentinel-1A constellation from the European Space Agency (ESA) was utilized to acquire SAR data. Images were taken a year since the start of operations of the said satellite in the Copernicus Program to maximize the area's documented ground deformation and movement. There were 153 images from October 2015 to December 2020, all in Interferometric Wide (IW) acquisition mode, C-band frequency, descending pass, and track number 163. The utilization of only descending pass images was realized during data download; limited ascending pass images that cover the study area are available. Also, only VV (vertical transmit, vertical receive) polarization was considered since such polarization provides higher coherence in selecting PS pixels [6-8]. Since the region of interest is a non-urban area with minimal presence of permanent structures, it is expected that the process will provide low PS density. Thus, images were segmented into 2015-2016, 2016-2017, 2017-2018, 2018-2019, and 2019-2020 to mitigate the risk of high decoherence. Master images for each duration were selected based on minimum temporal and perpendicular baseline [9].

A Shuttle Radar Topography Mission (SRTM) Digital Elevation Model (DEM) with a 1-arcsecond spatial resolution (30m) and 10-meter height accuracy was employed as external DEM, available at NASA Shuttle Radar Topography Mission Global 1 arc second V003. For validation purposes, the researchers utilized the available 1-m spatial resolution Light and Detection and Ranging (LiDAR)-derived Digital Terrain Model (DTM) acquired by the University of the Philippines-Diliman Phil-LiDAR 1 Program in the year 2014.

2.3. Image Pre-processing through SNAP

Subsequently, results were analyzed per event basis and the total of the six events (2017, 2018, June-2019, July-2019, 2020, & 2021) per cluster, barangay, and relating to Land Use/Land Cover (LULC) of the area. Moreover, spatial characteristic of high subsiding barangays was assessed regarding the location of the Philippine fault line segment near and along the area.

The Sentinel Application Platform (SNAP), an open-source toolkit, was utilized to process the SAR data. The python scripts snap2stamps [10] were implemented to automate the interferogram processing chain from a single master interferogram and to export pre-processed data for StaMPS PSI Analysis.

Master images must have maximum coverage of the region of interest (ROI), and TOPSAR-Split Operator was utilized to reduce the amount of downloaded SAR data. Processing parameters were set according to the settings of subswath, polarization, and bursts. Afterward, coregistration was done to utilize image statistics to align the slave images and the master at sub-pixel accuracy and create a master-slave stack. Once a stack is made, the phase difference can be determined. A stack of interferograms with elevation and orthorectified coordinates is generated by cross-multiplying the master image with the complex conjugate of each slave. Through the interferograms, specific information is gathered and is needed to estimate the target height and displacement point-by-point [11].

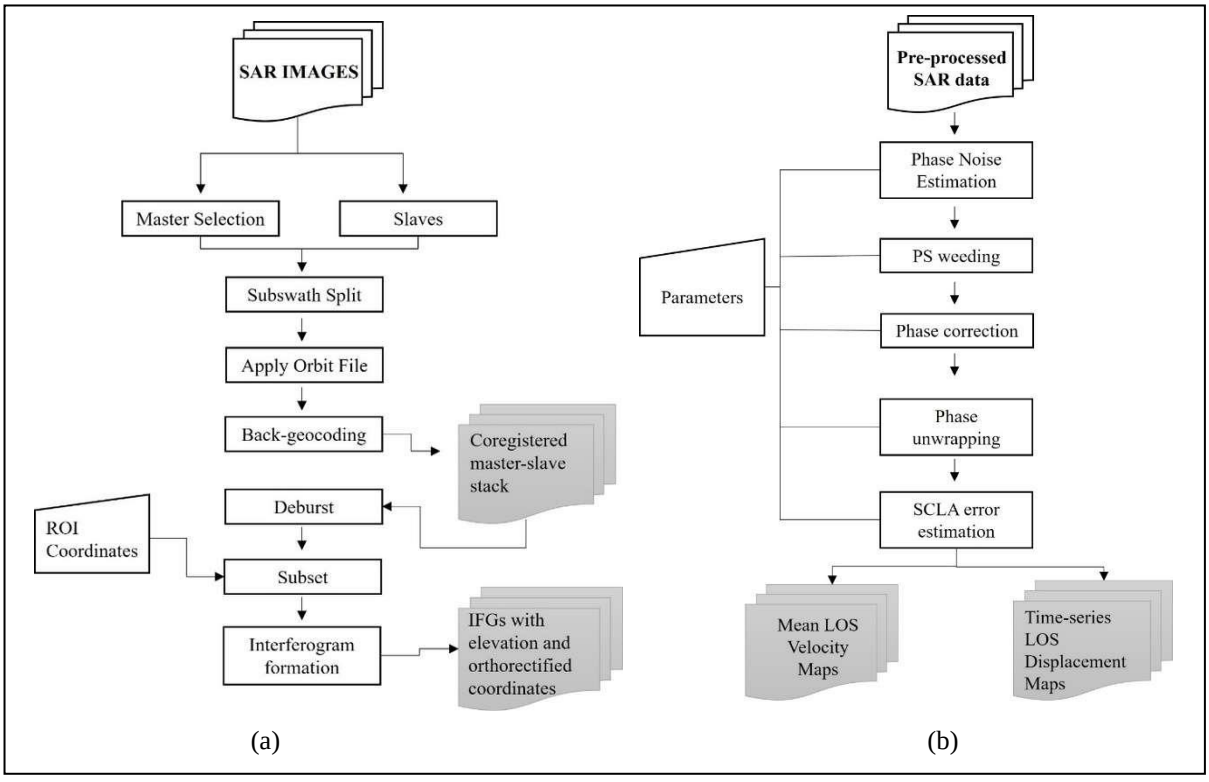

Figure 2 Workflow of the Study (a) for SNAP pre-processing and (b) StaMPS-MTI analysis processing chain

2.4. StaMPS – MTI Analysis

PS candidates were chosen based on their amplitude dispersion index (DA). DA describes the amplitude stability and acts as the basis to preselect pixels for phase analysis. The recommended range for DA is 0.4-0.42 since a higher threshold range will result in amplitude instability and low threshold results in low-density PS points. The temporal coherence of the scatterers was calculated by estimating the phase noise. Phase noise is approximately the residual

phase after the spatially correlated phase. Uncorrelated DEM errors are estimated and subtracted from the initial phase since PS pixels were chosen based on their phase noise characteristics. Although Sentinel SAR images have good incidence angle and polarization qualities suited for PSI analysis, PS points are also highly dependent on the 3D structure of the area. Thus, the study area's low PS points can be attributed to its lack of buildings and other engineering structures.

Using SNAPHU, the unambiguous phase is "unwrapped" from the wrapped phase. The ambiguity of the stacks is guided by selecting an available DEM in the SNAP toolbox. Phase measurements of PS-INSAR "wrap around" when observed motion exceeds half of the satellite's wavelength [12]. Furthermore, since this methodology assumes that the atmospheric phase is correlated in both space and time [13], a method called "phase unwrapping" is applied for atmospheric correction based on the wrapped phase and subtracts the phase uncorrelated in either space or time. This step produces an unwrapped image where estimated ambiguities and unclear and error-prone values are already removed. For comparison, the wrapped and unwrapped phases of images 2015-2016, respectively, are shown in the figures below.

The last step of StaMPS analysis can quantify the approximate DEM error and the atmospheric and orbit errors of the reference points. It also proves that although the final quantity of PS points used as a reference for the measurements is less than that of before it was weeded, the reference points contributed lesser error. The figure below shows DEM and orbits errors from unweeded PS with with 3782 PS pixels, and when weeded, having 1242 pixels.

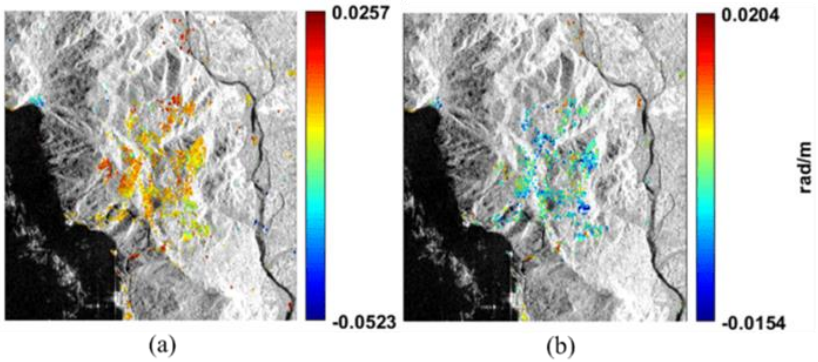

Figure 3 Map showing DEM and orbit errors from 2015-2016 with -0.0523 to 0.0257 rad/m and -0.0154 to 0.0204 rad/m, respectively.

3. RESULTS AND DISCUSSIONS

3.1. Line-of-Sight Mean Velocities

After running the steps and applying the parameters, the mean LOS velocities and corresponding standard deviation of each acquisition year are plotted below.

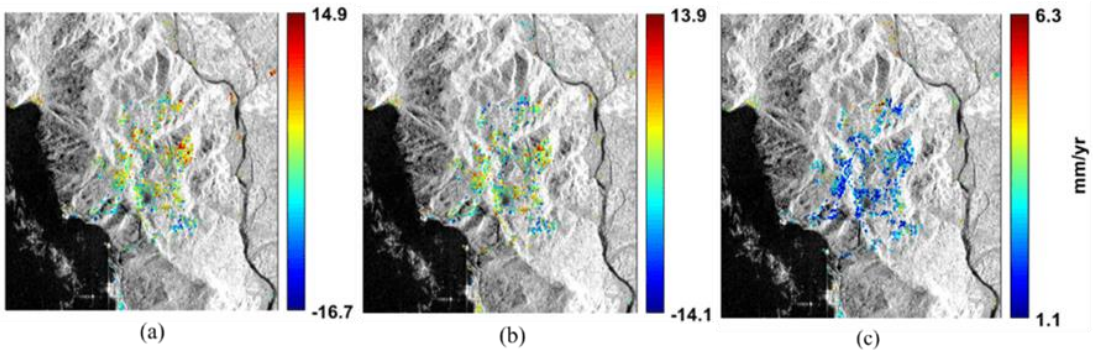

Figure 4 Deformation maps of 2015-2016 showing (a) mean velocities in satellite LOS without correction (b) corrected for topography-related and tropospheric phase delays (c) standard deviation estimated from the mean of all PS pixels

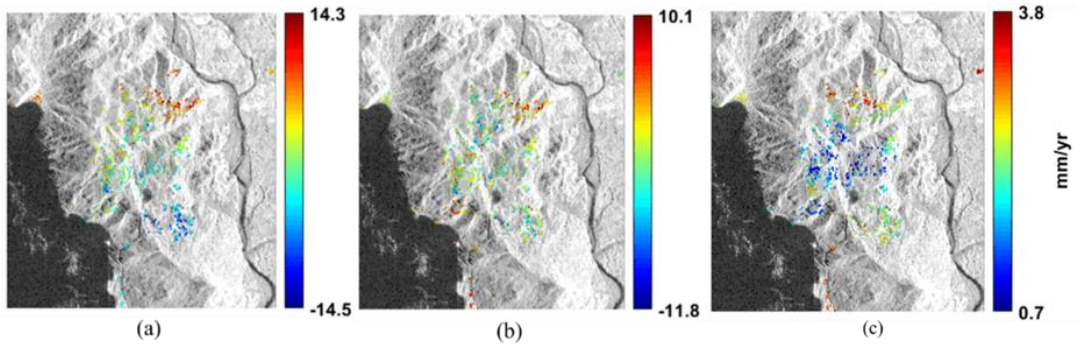

Figure 5 Deformation maps of 2016-2017 showing (a) mean velocities in satellite LOS without correction (b) corrected for topography-related and tropospheric phase delays (c) standard deviation estimated from the mean of all PS pixels.

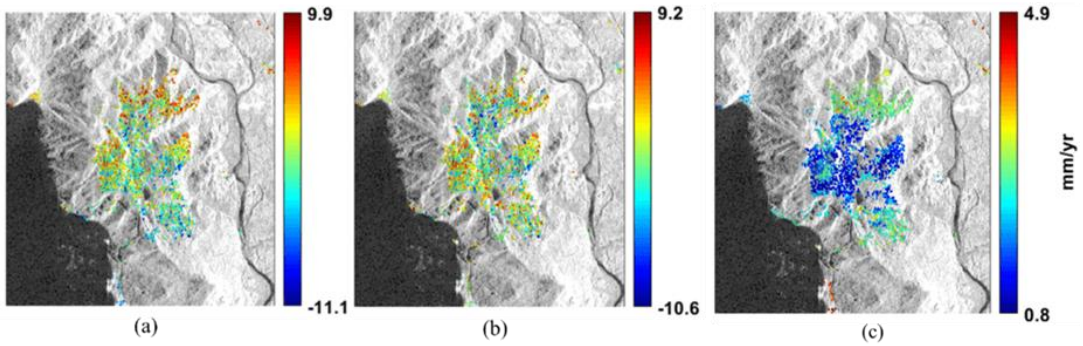

Figure 6 Deformation maps of 2017-2018 showing (a) mean velocities in satellite LOS without correction (b) corrected for topography-related and tropospheric phase delays (c) standard deviation estimated from the mean of all PS pixels

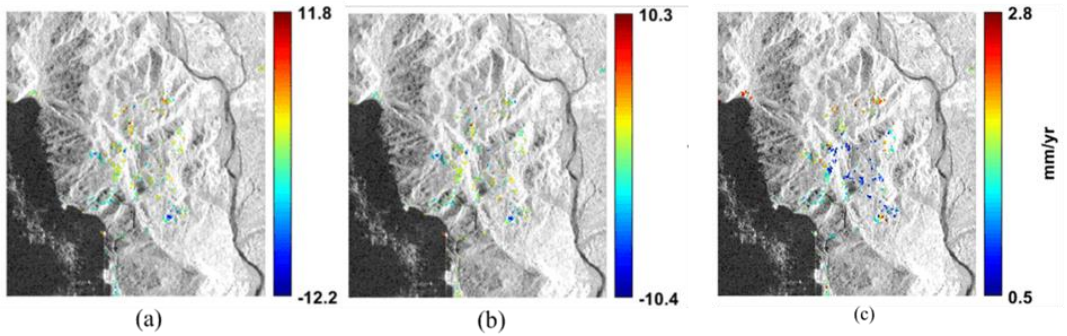

Figure 7 Deformation maps of 2018-2019 showing (a) mean velocities in satellite LOS without correction (b) corrected for topography-related and tropospheric phase delays (c) standard deviation estimated from the mean of all PS pixels.

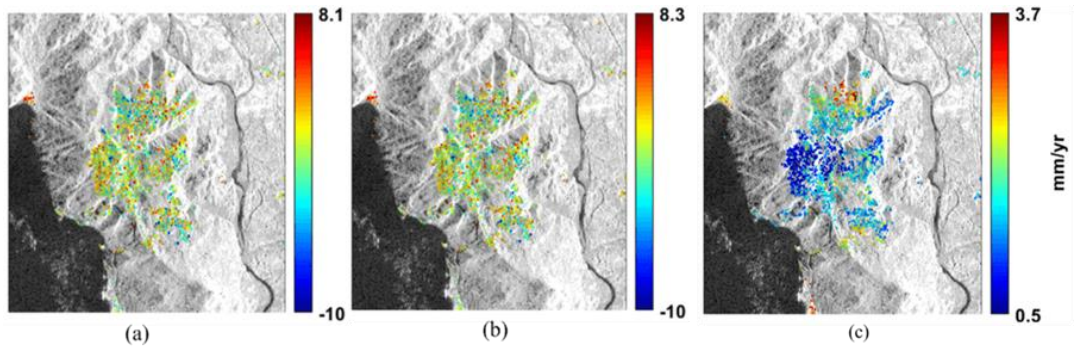

Figure 8 Deformation maps of 2019-2020 showing (a) mean velocities in satellite LOS without correction (b) corrected for topography-related and tropospheric phase delays (c) standard deviation estimated from the mean of all PS pixels

Outputs show movements relative to the mean of the whole area, where negative values indicate movement away from the satellite, depicting subsidence, whereas positive values mean uplift. The series of maps shows a trend where the upper part of the study area from 2015-2020 has constant uplifting quality but again in decreasing manner. Displacement values of the mining area range from approximately ± 8mm/yr to ± 14mm/yr. The 2018-2019 and 2019-2020 datasets have the two highest PS pixels and have shown the slightest difference between the initial and corrected mean velocity. Table 1 presents that both the values for subsidence and uplift are decreasing.

Table 1 Consolidated results of PS-InSAR, values in mm/year

Year	Mean Velocity	Corrected Mean Velocity	Standard Deviation
2015-2016	-16.7280 to 14.9015	-14.0936 to 13.9462	1.06017 to 6.30855
2016-2017	-12.2414 to 11.8478	-10.3907 to 10.3434	0.497861 to 2.80087
2017-2018	-14.5063 to 14.2571	-11.8255 to 10.0755	0.720226 to 3.83996
2018-2019	-11.055 to 9.88815	-10.5639 to 9.15925	0.82712 to 4.83256
2019-2020	-10.0076 to 8.09264	-10.021 to 8.32193	0.478571 to 3.67554

For the earlier years, areas with subsidence are more focused on the lower part but are being dispersed in the later years. It can be assumed that the upper part is being used as a dumping site for the removed materials. The lower portion must have been the primary mineral exploitation and excavation area. Moreover, displacement values of the PS pixels show a significant decrease over time, where mean velocity values are mainly within the range interval's mid-portion (green to yellow-green). Furthermore, based on the decreasing determined mean velocities of the area, it is very likely that the intensity of mining activities from 2015 until 2020 has lessened. Such assumptions can be tested by determining the actual mining activities conducted by the company in the area.

The processing chain proved reliable and valuable in quantifying displacements of the area. Mining companies can utilize the method to assess the deformation their activities have caused. Local government units can further improve and use the technique of monitoring Caraga Region mining companies. Overall, the values of displacements present in San Roque Mining Incorporation in the 2015-2020 period are not alarming and are less likely to cause significant deformation. However, the mining area had been in constant and continuous deformation for a long time, although minimal; thus, deformation assessment studies on the mining area are vital to determine further the degree of deformation and how it can impact surrounding communities.

3.2. Time Series Deformation

Before analyzing the generated time-series displacement maps, the researchers selected a persistent scatterer on the central portion of the study area, having the highest subsidence value. For the consistency of the datasets, the exact coordinates (9.2036ºN, 125.5369ºE) of the selected pixel point were used to visualize the time-series displacement maps from 2015 to 2020. Researchers can choose a different PS pixel or input a pre-determined coordinate if external information can be used as a reference point.

It is worth noting that the specified area has a subsiding characteristic in 2015-2016, shown in a downward trend, but has an upward trend for the rest of the acquisition year. It can also be seen in the mean velocity figures 13-17 that the reference point was initially tagged as red (subsidence value) but for the following years, colored as light yellow-light green. This measuring technique can help determine the behavior of a specific point or a comparing series of points.

Figure 9 (d) exhibits the most stable displacement among the rest of the datasets. This stability may be a by-product of its low standard deviation since the 2018-2019 dataset has the highest PS pixels.

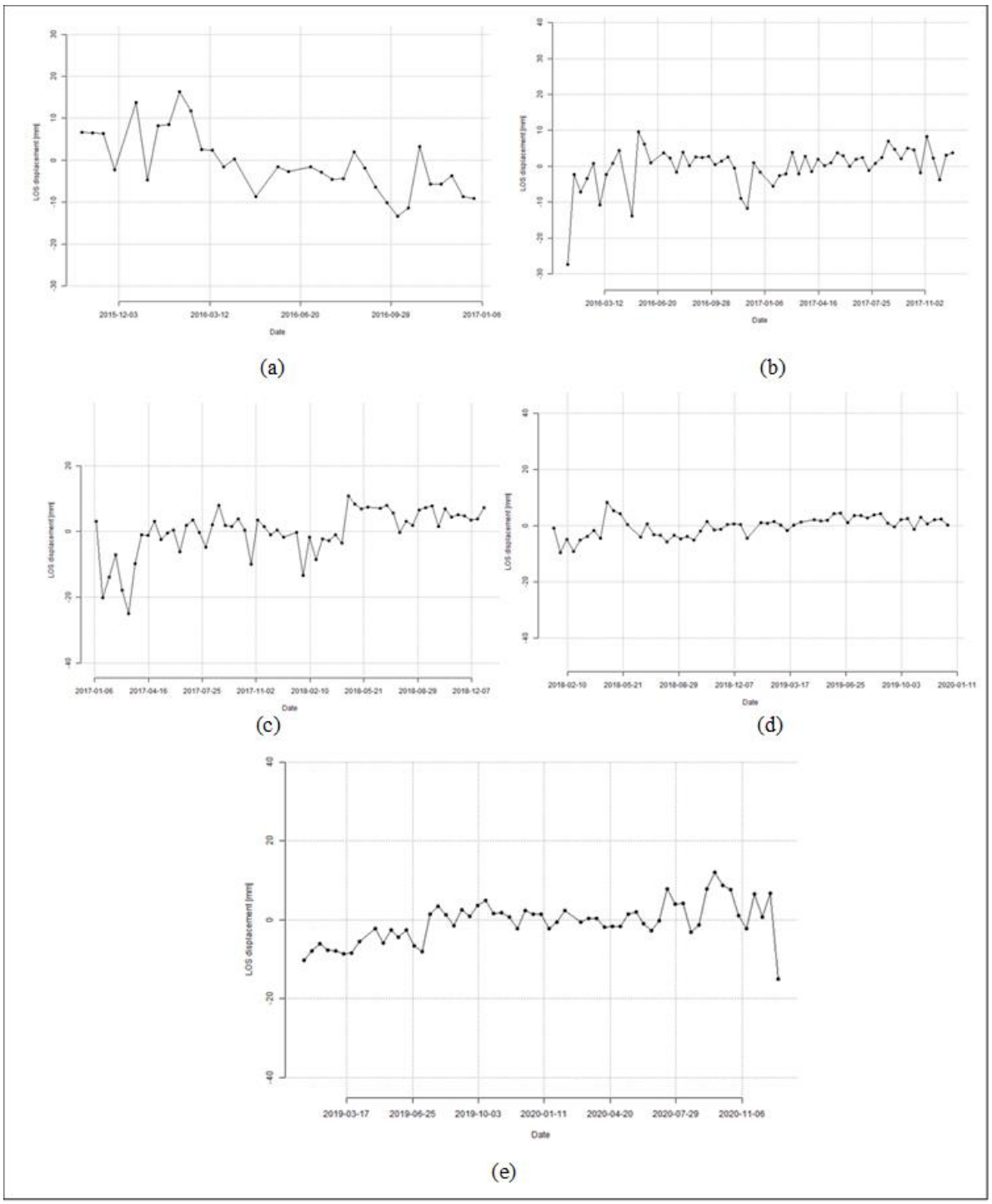

Figure 9 Time series displacement of year (a) 2015-2016 (b) 2016-2017 (c) 2017-2018 (d) 2019-2020 and (e) 2020-2021 with 4000-m radius.

3.3. Validation

Fifty (50) PS pixels that were found to have low mean velocities in the 2015-2016 dataset were used for validation. These pixels have mean velocities within ± 1 mm/yr and are the areas that have shown to have minimal changes or movement. Elevation values have an RMSE of ~4.85 meters and a standard deviation of ~4.52 meters. However, the coefficient of determination (R2) has a good value of 0.9952. The high RMSE could be primarily caused by the vast gap between the acquisition dates of the data used to generate the LiDAR DTM (2014) and the S-1 images used for the 2015 DEM. The LiDAR DTM used had a much greater resolution, 1-m, than the generated DEM with a 20-m spatial resolution. Also, there is a significant possibility that ground deformation movements from 2014-2015 in the mining site cannot be documented by the satellite. A solution for this is integrating other satellites that have been in operation longer than Sentinel-1.

4. CONCLUSIONS AND RECOMMENDATIONS

The utilization of StAMPs/MTI Analysis as a processing chain for time-series ground deformation monitoring and to test its applicability and functionality, based on the outputs generated, was a success. However, a few parameters were changed since this methodology is opportunistic to different mining settings. The process generated reasonable values for line-of-sight mean velocities and time-series displacement maps even though the PS pixels were limited. Parameters that greatly influence the outputs, such as amplitude dispersion index and neighbor weeding, resulted in a low number of PS pixels but generally lesser orbit errors and standard deviation. The 2018-2019 and 2019-2020 datasets have the highest PS pixel numbers and provide the most stable mean velocity results. This suggests that the parameters involved can perform more excellently with an increased presence of persistent scatterers.

The 2015-2020 datasets show subsidence and uplift phenomena with an approximate value of ±10 mm per year. The earliest data suggests dumping activities in the upper mining area and excavation in the lower part. While, the time-series movement of the reference point, located at the central portion of the mining area, showed subsidence from 2015 to 2016 and uplift in the rest of the datasets. Although actual mining activities were not sourced and are unknown, mining activities such as dumping and excavating in specific areas can be mapped out, predicted, and monitored through this methodology.

StaMPS/MTI analysis was proven influential in determining ground movement up to millimeter accuracy, even if the study area was not optimal for such a processing chain due to the minimal presence of PS pixels. This method can be used to monitor or assess ground movements and deformations. In addition, partitioning time-series studies into shorter sets of acquisition years and imposing stricter parameter thresholds, especially in urban areas, can maximize the presence of persistent scatterers.

To further improve future related studies, the following are the recommendations of the researchers:

- Try to integrate both descending and ascending tracks to produce vertical displacements.
- Conduct actual ground survey around the mining site, if possible, for validation of the outputs

5. REFERENCES

[1] D. B. Gesch, "An inventory of topographic surface changes: The value of multitemporal elevation data for change analysis and monitoring," International Archives of the Photogrammetry, Remote Sensing and Spatial Information Sciences - ISPRS Archives, vol. 40, no. 4, pp. 59–63, 2014, doi: 10.5194/ISPRSARCHIVES-XL-4-59-2014.

[2] A. E. Maxwell, M. P. Strager, A. E. Maxwell, and M. P. Strager, "Assessing landform alterations induced by mountaintop mining," Natural Science, vol. 5, no. 2, pp. 229–237, Feb. 2013, doi: 10.4236/NS.2013.52A034.

[3] A. Lazarov, D. Minchev, and C. Minchev, "InSAR Modeling of Geophysics Measurements," Geographic Information Systems in Geospatial Intelligence, Nov. 2019, doi: 10.5772/INTECHOPEN.89293.

[4] M. Crosetto, O. Monserrat, M. Cuevas-González, N. Devanthéry, and B. Crippa, "Persistent Scatterer Interferometry: A review," ISPRS Journal of Photogrammetry and Remote Sensing, vol. 115, pp. 78–89, May 2016, doi: 10.1016/J.ISPRSJPRS.2015.10.011.

[5] "Agusan Norte officials, town folk urge nickel miner to go | GMA News Online." https://www.gmanetwork.com/news/news/regions/207565/agusan-norte-officials-town-folk-urge-nickel-miner-to-go/story/ (accessed Dec. 05, 2021).

[6] "(PDF) Comparison of HH and VV Polarizations for Deformation Estimation using Persistent Scatterer Interferometry." https://www.researchgate.net/publication/321251393_Comparison_of_HH_and_VV_Polarizations_for_Deformation_Estimation_using_Persistent_Scatterer_Interferometry (accessed Dec. 14, 2021).

[7] Z. Sadeghi, M. Javad Valadan Zoej, A. Hooper, S. Member, and J. M. Lopez-Sanchez, "A New Polarimetric Persistent Scatterer Interferometry Method Using Temporal Coherence Optimization; A New Polarimetric Persistent Scatterer Interferometry Method Using Temporal Coherence Optimization," 2018, doi: 10.1109/TGRS.2018.2840423.

[8] E. Bedini, "Persistent Scatterer Interferometry of Sentinel-1 time series to detect ground subsidence in the city of Recife, Brazil," Journal of Hyperspectral Remote Sensing, vol. 10, no. 1, pp. 1–9, May 2020,

Accessed: Dec. 14, 2021. [Online]. Available: https://periodicos.ufpe.br/revistas/jhrs/article/view/243974

[9] A. Hooper, P. Segall, and H. Zebker, "Persistent scatterer interferometric synthetic aperture radar for crustal deformation analysis, with application to Volcán Alcedo, Galápagos," Journal of Geophysical Research: Solid Earth, vol. 112, no. B7, p. 7407, Jul. 2007, doi: 10.1029/2006JB004763.

[10] J. M. D. Blasco and M. Foumelis, "Automated SNAP Sentinel-1 DInSAR processing for StaMPS PSI with open source tools," Jul. 2018, doi: 10.5281/ZENODO.1322353.

[11] M. Gao et al., "Land Subsidence and Ground Fissures in Beijing Capital International Airport (BCIA): Evidence from Quasi-PS InSAR Analysis," Remote Sensing 2019, Vol. 11, Page 1466, vol. 11, no. 12, p. 1466, Jun. 2019, doi: 10.3390/RS11121466.

[12] B. Osmanoğlu, F. Sunar, S. Wdowinski, and E. Cabral-Cano, "Time series analysis of InSAR data: Methods and trends," ISPRS Journal of Photogrammetry and Remote Sensing, vol. 115, pp. 90–102, May 2016, doi: 10.1016/J.ISPRSJPRS.2015.10.003.

[13] H. Yang, J. Liu, J. Peng, J. Wang, B. Zhao, and B. Zhang, "A method for GB-InSAR temporal analysis considering the atmospheric correlation in time series," Natural Hazards 2020 104:2, vol. 104, no. 2, pp. 1465–1480, Aug. 2020, doi: 10.1007/S11069-020-04228-W.